

Recovering Historical Film Footage by Processing Microtomographic Images

Chang Liu^{1,2}, Paul L. Rosin², Yu-Kun Lai²,
Graham R. Davis³, David Mills³, and Charles Norton⁴

¹ School of Astronautics, Beihang University, China

² School of Computer Science & Informatics, Cardiff University, UK

³ Institute of Dentistry, Queen Mary University of London, UK

⁴ BBC Archive Development, UK

Abstract. 1960s film was typically printed on tri-acetate film base. If not preserved properly, such material breaks down at a chemical level, which is a non-stoppable process that permanently fuses the film so that it essentially becomes a lump of solid plastic. Recently, some precious films, such as the only known copy of the earliest surviving episode of ‘The Morecambe and Wise Show’ have been discovered, but they are in poor condition. They will eventually turn into a pool of sticky liquid and be gone forever. In this paper, as proof of concept, we use X-ray microtomography to provide 3D imaging of a test film of similar vintage, and propose an automatic method to extract footage from it.

Keywords: tri-acetate film, X-ray microtomography, 3D imaging

1 Introduction

In 1968, Eric Morecambe and Ernie Wise came to London to make a new light entertainment series for BBC 2, which would come to dominate the UK light entertainment landscape for the next 15 years. Sadly, the BBC never formally archived that very first season of ‘The Morecambe and Wise Show’. Before the advent of commercial video exploitation (DVDs, iplayer etc.), bodies like the BBC saw little purpose in maintaining a large and expensive collection of programming. ‘The Morecambe and Wise Show’ (like almost all UK comedy broadcasts of the time) was recorded to and transmitted from videotape. After being broadcasted, the master-tape would be stored for a limited period of time for potential re-use and eventually cleared for wiping.

A programme *might* still survive, but only if it was deemed likely to be popular overseas. Around the time of broadcast, many BBC programmes would also be copied to 16mm black and white film via a process called telerecording. A master-tape would be played on a special flat cathode ray tube screen. A 16mm film camera was pointed at this screen and filmed the programme. These film recordings were made for international syndication, and, since most countries were able to play 16mm film, this became the standard format for the marketing of BBC programmes overseas.

All of the episodes of that first season of ‘The Morecambe and Wise Show’ were telerecorded to black and white film. Rather than having multiple film prints created for each episode, it was routine for prints to be shared. When the episodes had been screened by everyone who wanted them, the last network in the chain would be asked to send the film back to BBC Enterprises in London or for the films to be destroyed (to stop them being screened without permission). By the late 1970s, series one of ‘The Morecambe and Wise Show’ had reached Nigeria, in the film stores of a broadcaster called RKTВ.

At some point prior to 1978 BBC Enterprises decided that there was no need to retain their black and white negatives of ‘The Morecambe and Wise Show’ since colour television had become established across the world. They destroyed the films, and along with the destruction of their master-tapes some years before, this now meant that the BBC no longer held any recordings of the first series of ‘The Morecambe and Wise Show’.

Then in 2012, a freelance film researcher called Philip Morris gained rare access to the RKTВ vault, which consisted of a hot, poorly ventilated outbuilding in a small settlement called Jos in the heart of Nigeria. The area suffers from high-humidity in the rainy season and a desert of drought at all other times. The often poor state of the films in the archive reflects these harsh conditions. Philip Morris’ trip to the RKTВ vault was worthwhile, as it turned out RKTВ held unique film recordings of various BBC programmes that were not known to exist elsewhere in the world, including episodes of both ‘Doctor Who’, ‘The Sky at Night’ and finally also ‘The Morecambe and Wise Show’. RKTВ now retained only one episode of ‘The Morecambe and Wise Show’, but it was still an important find. On a single 16mm film spool, RKTВ had the earliest surviving episode of ‘The Morecambe and Wise Show’ and the earliest surviving footage of the double act working for the BBC.

However, there was a problem: the Nigerian Morecambe and Wise film was in an advanced state of decay. The episode was on a form of film stock (i.e. the flexible ribbon of transparent plastic backing onto which the image is printed) not used nowadays called cellulose acetate, and was suffering from ‘tri-acetate film base degradation’ – a film ‘disease’ that can cause film to rot away to nothing. If kept in humid conditions for any prolonged period of time, the tri-acetate can begin to break down at a chemical level, leading to a runaway reaction. At a molecular level, as the plastic increases in temperature, the acetate breaks down releasing a vapour of acetic acid, which further breaks down the plastic by eating away at the film, through general acidic corrosion. The process only stops when there is no more acetate left to be converted [4].

The RKTВ Morecambe and Wise film had been stored in exactly the wrong sort of conditions for an acetate roll: a humid atmosphere with poor ventilation and a cracked film can that did not shield the film from sunlight. As the acid has eaten away at the surface of the film, the roll has become sticky, thinner and lacking in overall structural integrity. Every layer of film on the Morecambe and Wise roll has now permanently fused itself with every adjacent layer of film, so that all of the pictures are now sealed inside a solid lump of plastic. Since

the film is sitting in a self-sustaining vapour of corrosive acid, eventually this priceless roll will turn into soup. There is nothing we can do to stop that rot.

The BFI film archives recommended its destruction since the sheer quantity of acid vapour being produced by the film made it a hazard to other rolls in the BFI's collection. The risk of 'infection' is always high with this kind of stock.

There is a long history of film restoration [1], and many techniques have been developed [6, 7]. Much of that work involves applying image processing techniques to enhance existing footage, whereas for the Morecambe and Wise film that footage needs to be first recovered from the acetate roll. In this paper we describe a radically different approach to dealing with the film, inspired by work in other areas of culture heritage.

In 2012, archaeologists embarked on a project to examine the Antikythera mechanism – a Greek navigational calculator constructed around the end of the second century BC. High-resolution X-ray tomography enabled them to analyse the inner workings of the device, without breaking the item apart [5]. Recently, several of the authors of the current paper have worked on the task of reading historical scrolled parchment documents which have been damaged due to fire or water. Such damage makes the document fragile, and often impossible to open without causing considerable further damage. It was demonstrated that using high-resolution X-ray tomography it was possible to virtually unroll a parchment from the X-ray volume, and recover its written contents [9].

Any roll of film is essentially just a strip of plastic with a picture printed onto one side of it, which for a monochrome image is always applied in the same basic way. The image layer is called the emulsion layer and the key component of black and white emulsion is silver oxide. The metal content in silver oxide emulsion is very high. This suggested that it should be possible to apply X-ray microtomography to obtain images from a roll of black and white film.

As a study of feasibility, in this paper we use the film of 'Snow White and the Seven Dwarfs', a black and white film on tri-acetate stock of roughly the same vintage as 'Morecambe and Wise'. It was an 8mm silent black and white digest print from the 1970s containing the 1965 American dubbed version of the 1955 German film 'Schneewittchen'. We first introduce how the film was scanned and some early effort to construct the footage, which involved user interaction. We then introduce a novel *automatic* algorithm to reconstruct the footage. This is followed by experimental results and discussions.

2 Film Scanning and Early Effort of Reconstruction

Prior to tomographic scanning, a single thickness of 8mm silent black and white film (extracted from Snow White) was X-rayed at 40kV and 405 μ A, using a 0.5 mm Al filter. Although this X-ray energy was far too high for optimal contrast, it was necessary in order to penetrate even a small roll of film. The MuCAT 2 X-ray microtomography scanner at Queen Mary University of London [2] was used, which employs time delay integration to obtain very high contrast images. But even with an equivalent exposure time of 40 seconds, little image contrast

could be seen. Given the poor image contrast, a long exposure time was set for the tomographic scan. This was also performed at 40 kV and 405 μA . A length of the film was rolled and inserted into a 27mm internal diameter plastic container. 2115 projections were recorded with an equivalent exposure time of 20 seconds per projection to ensure a high SNR. The voxel size was 20 μm .

The reconstructed film scan showed good signal to noise ratio. Streak artefacts were present, due to tangential X-ray paths passing through relatively long lengths of silver. For future scans, these can be reduced in severity by increasing the number of projections (the exposure time can be reduced to keep the same total acquisition time).

The recent work in [3] demonstrated the possibility of recovering footage from XMT scanned data. The method however requires manual interaction and assumes uniform structure of the film. Moreover, it would be difficult to generalise such methods to a highly damaged dataset.

3 Method for Image Recovery from Film

In this work, we will describe an *automatic* approach to footage recovery. We first introduce the method to recover the image printed on the film and in the next section, the method to create the video footage from such images.

3.1 Preprocessing and Initialisation

An example slice of the Snow White film is shown in Fig. 1. It looks similar to parchments which our previous research has developed several effective methods to deal with [10, 9, 8]. However, the methods for parchment unrolling fail on this data because they assume that the parchment layers are mostly separated by at least a small gap, whereas the film is more tightly rolled. On the other hand, film is more uniform than parchment. Thus, in this work we focus on modelling the appearance of the film, for which we use image intensity ridges [11], while making no assumptions about any background gaps. Ideally, the ridges should form a continuous spiral curve, but they are often incomplete. There also exist artifacts, false positive responses which should be discarded. Based on the fact that adjacent slices have similar images and hence similar ridge locations, we semi-automatically correct the first slice, and automatically propagate the ridges across slices, using the previous slice to constrain the linking of the next slice.

3.2 Propagation

Because of the large similarity between two adjacent images, if the ridge sections in the previous image have been correctly linked, so that there exists an entire ridge in the previous image, we can use the previous ridge image as a reference to connect the ridge sections in the current image. In Fig. 2(a), the blue spiral represents the previous ridge, i.e. the reference ridge, the red curves are some ridge fragments in the current image. Generally, if a fragment is a section of the

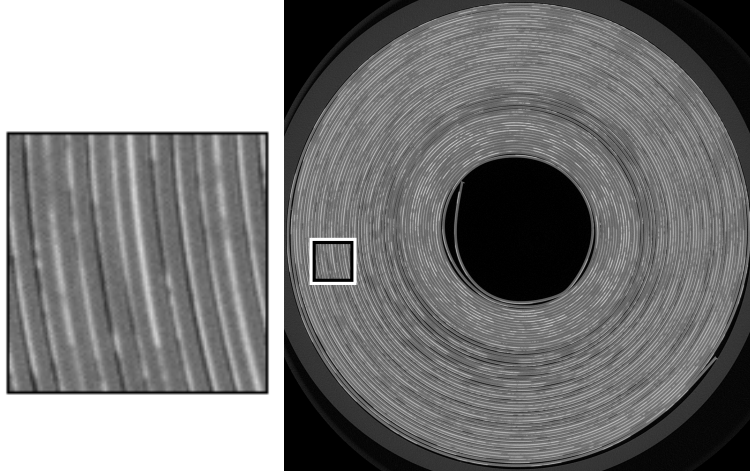


Fig. 1. An X-ray image of Snow White film. A section is shown zoomed in.

film ridge rather than an artifact, it should be very close to the reference ridge. By means of this condition, we check whether a fragment is a ridge part or not in the following way. Let points v_1 and v_2 be the two endpoints of a fragment and their nearest points on the reference ridge be points p_1 and p_2 respectively. l_1 is the length of the path p between p_1 and p_2 on the reference ridge; l_2 is the length of the fragment, and d_i is the distance between v_i and p_i , $i = 1, 2$, and t_1 and t_2 are thresholds. We will consider this fragment as an artifact instead of a ridge section, thus deleting this fragment if one of the following conditions is true: $\max\left(\frac{l_1}{l_2}, \frac{l_2}{l_1}\right) > t_1$, or $d_1 + d_2 > t_2$. The former states that the lengths l_1 and l_2 differ too much and the latter states that the endpoints of the fragment are too far away from the closest ridge. Otherwise, we will keep the fragment, and delete the pixels between p_1 and p_2 along p . After dealing with all the fragments in the current image, the reference ridge becomes the form shown in Fig. 2(b). It can be readily found from Fig. 2(b) that the original entire reference ridge has been broken into several segments, and it is noteworthy that the two endpoints of two different fragments in the current image should be linked only if their nearest points on the reference ridge are the endpoints of the same segment. Therefore we can merge the ridge parts in the current image together using this criterion.

3.3 Linking Method

Based on the aforementioned criterion, we can easily select the two endpoints which should be linked and then connect them by a curve parallel to their adjacent ridge. First of all, we find the closest ridge for each endpoint. As illustrated in Fig. 3, given an endpoint p_i , a line which passes through p_i and is perpendicular to the orientation at p_i meets the upper closest ridge at m_i , and the lower closest ridge at n_i . The ridge where m_i or n_i lies are the closest ridge of p_i . Providing that there exist two endpoints p_i and p_j which ought to be linked,

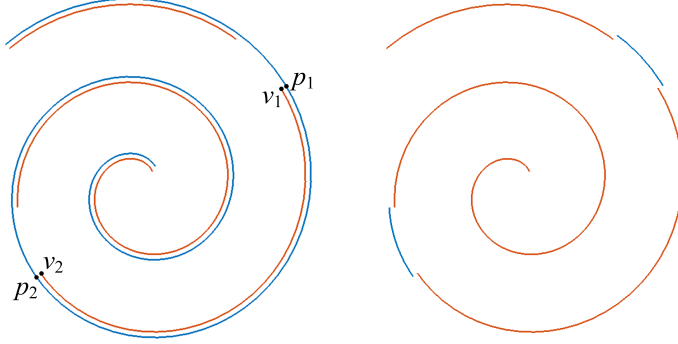


Fig. 2. Determining which two endpoints should be linked. (a) The previous ridge image and the current ridge image. (b) The endpoints in current image whose nearest points on the reference ridge are the two endpoints of a segment should be linked.

they can be linked on condition that they have at least one same closest ridge. As depicted in Fig. 3, p_i and p_j have two same closest ridges. We first generate a curve Q_1 which is as parallel to curve m_im_j as possible to connect p_i and p_j , and then check if this curve intersects the existing ridges at any places other than p_i and p_j . If not, Q_1 can be used to link p_i and p_j together, so if p_i and p_j only have one same closest ridge, we will connect p_i and p_j by Q_1 and then begin to check other endpoint pairs. If p_i and p_j have another same closest ridge, as shown in Fig. 3, we will use n_in_j to generate another as-parallel-as-possible curve Q_2 in the same way, and evaluate Q_1 and Q_2 by the following equation:

$$H_1 = 1 - \frac{\min(m_ip_i, m_jp_j)}{\max(m_ip_i, m_jp_j)}, \quad H_2 = 1 - \frac{\min(n_ip_i, n_jp_j)}{\max(n_ip_i, n_jp_j)}. \quad (1)$$

Eq. 1 reflects the similarity of the distances from p_i and p_j to their closest ridge. The smaller H_1 (respectively H_2) means p_i and p_j are at a more similar distance to m_im_j (respectively n_in_j) than to n_in_j (respectively m_im_j), so it is more suitable to use the curve generated from m_im_j (respectively n_in_j) to link p_i and p_j . Eventually the curve which has smaller H -value will be chosen to connect p_i and p_j together. We repeatedly use this algorithm to process all pairs of endpoints which should be linked until no pair of endpoints should be linked in the current image.

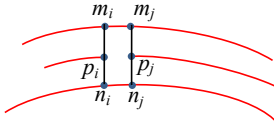


Fig. 3. Linking the two endpoints which should be linked.

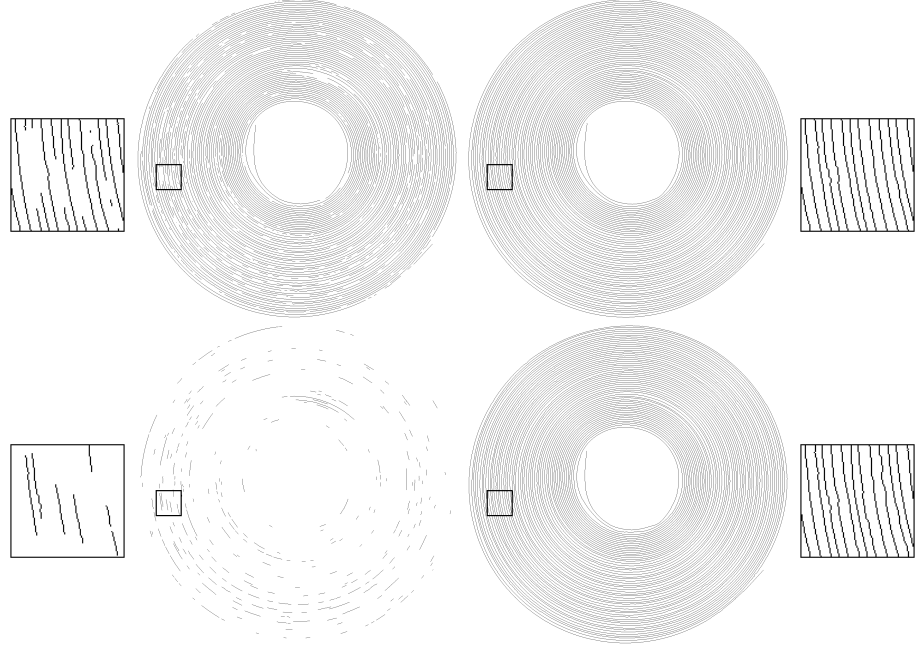


Fig. 4. Getting the entire ridge. (a) The current ridge image. (b) The previous ridge image. (c) An intermediate result. (d) The final result.

3.4 Ridge Propagation Result

We show a result of ridge propagation. We set $t_1 = 4$ and $t_2 = 10$ in our experiments. The current ridge image (Fig. 4(a)) consists of many fragments. The reference ridge image, i.e. the previous ridge image, is shown in Fig. 4(b). These are used by the propagation method in Section 3.2 to produce the result in Fig. 4(c). The endpoint pairs in Fig. 4(a) corresponding to the two endpoints of a segment in Fig. 4(c) are connected by the method in Section 3.3. The final result is displayed in Fig. 4(d), in which all the fragments in Fig. 4(a) have been correctly merged together, producing an entire film ridge in the current image.

Once the ridges are recovered, we use the ink projection method in [10, 8] to obtain a flattened image, which contains all the frames of the footage (see Fig. 5(top)). Since the ridges contain the footage frames, when performing projection only a thin layer close to the ridges need to be considered (the maximum displacement in either direction is set to 2 pixels).

4 Extracting Frames

Once the reconstructed image containing the film strip has been obtained, the final task is to extract the individual frames so that they can be reassembled as a video. As can be seen in Fig. 5a there is an approximately sinusoidal oscillation, the period of which increases by a factor of about 2.7 from the beginning to

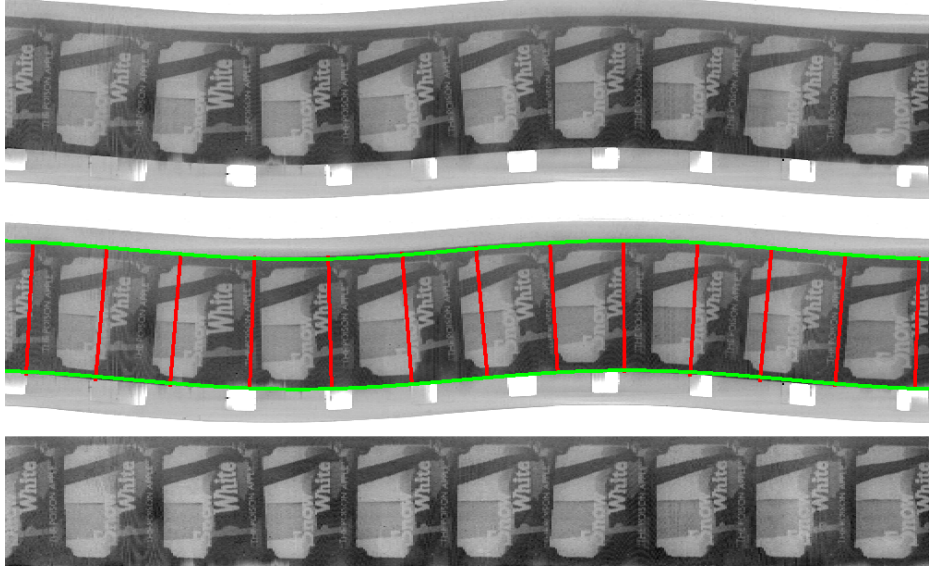


Fig. 5. Straightening a section of reconstructed film strip. a) initial reconstructed film strip showing sinusoidal deformation, b) sinusoid fitted to the boundary curves (shown in green) and sampled normals (shown in red), c) film strip after warping and cropping.

the end of the reconstructed film strip. This oscillation is due to the film not being aligned perfectly vertically when placed in the X-ray scanner, while the increasing period is a consequence of the spiral roll of the film. To simplify subsequent processing, the film strip is straightened to correct for the oscillation.

First, the boundaries of the central part of the film strip that contains the images is extracted. Since the area of the image outside this area is relatively bright a simple approach is sufficient. The height H of a single frame⁵ is manually determined, and then for each column in the image the range $[i_c, i_c + H]$ that minimises the summed intensities $i_c = \text{argmin}_r \sum_{r=i}^{i+H} I[r][c]$ is considered as the frame. The set of frame boundaries $i_c; c = 1 \dots n$ provides the upper boundary for the film strip. Since each point along the boundary is estimated independently, they can be noisy, so robust smoothing is applied to the boundary which down-weights the effect of outliers.

The boundary is modelled as piecewise sinusoidal (with a fixed frequency per section). Since a sinusoidal function is non-linear, fitting to data tends to be unreliable unless a good initialisation is provided. The amplitude is already known from the height H of a single frame, and the mean height of the boundary curve provides the offset. The frequency is determined by computing the autocorrelation of the sampled boundary function, and finding the lag that produces the

⁵ Height H refers to the height of the frame which is in the film strip, and is therefore rotated 90° to the normal viewing position.

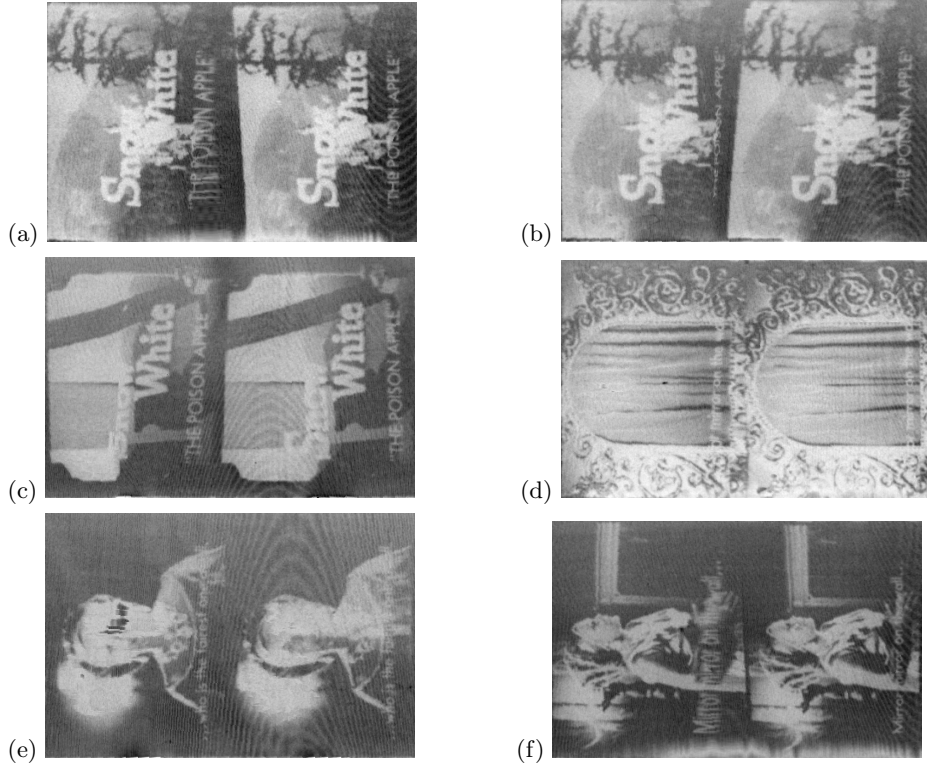


Fig. 6. Examples of problems for segmentation of film strip into frames. a) nonlinear stretching of frame, b) nonlinear compression of frame, c) first frame smaller than second frame, d) two frames with weak frame boundary, e) first frame contains reconstruction artifact, f) bright patches.

first peak in the autocorrelation function. Finally, the first peak in the boundary function is detected, providing the phase.

This procedure is applied to small sections (5000 pixels long) of the film strip to estimate the upper boundary curve. The lower boundary is taken as the same curve vertically shifted by H . Fig. 5b shows the fitted curves for a part of a section. A sparse set of corresponding points are found in the upper and lower curves by computing the normals from the sinusoidal function, and projecting them from the upper curves towards the lower curves. A thin plate spline warp is applied to the image using the endpoints of the normals in the source image which are mapped to a set of vertically aligned normals, separated by the arc-length along the sinusoid, in the target image. Fig. 5c shows the warped image (after cropping) which has effectively straightened that section of the film strip. The results for the individual sections are concatenated back to form a single 150336×281 pixel image.

Once the film strip has been straightened and cropped it should be straightforward to split the image into frames. However, in practice this is problematic



Fig. 7. Extracting frames. The green lines indicate estimated regular frame boundaries, while the red lines show the keyframes that were determined to start a new shot. The extracted frames are shown below after resizing to a common width

due to several factors. First the process of recovering the film strip from the XMT image volume introduces nonlinear deformations in the geometry. Examples can be seen clearly in Fig. 6, in which parts of the image are stretched (see Fig. 6a) or compressed (see Fig. 6b). As a consequence, the frames have been sheared, so that the vertical frame border has become diagonal. Fig. 6c shows a pair of frames in which there has been a 10% change in width. In addition, the image quality is poor. Not only are the images noisy and low resolution (213×281 pixels), but there are several types of artifacts:

- Due to the partial volume effect banding is visible in many of the frames in Fig. 6. The curved film surface results in the curvature of the bands.
- Fig. 6e shows an example of image reconstruction errors (in the face).
- At the edges of frames there are sometimes some bright patches, e.g. Fig. 6a&f. The film tends to be a little wrinkled at the edges, and consequently these are also manifestations of the partial volume effect.

Finally, the boundary between frames is often not evident. For instance in Fig. 6d&e most of the boundary does not contain any significant vertical discontinuity in intensity or texture.

To split the film we provide the width W of the first frame F_1 in the film strip. All other frames will be resized to this width. The next frame F_2 is assumed to follow, but may have width $W \pm w$. The set of possible frames F_2 are compared against F_1 and the one maximising a normalised cross-correlation score is selected. Once frame F_i is found it is used to estimate the width of the next frame F_{i+1} . In addition, a threshold on the normalised cross-correlation score is used to check that the match is sufficiently good. Otherwise there may be substantial

distortion between frames F_i and F_{i+1} . Alternatively, there could be substantial change in appearance between the frames, either from a fast moving object, sudden changes in lighting, or a cut between scenes. This would make the estimation of the width of F_{i+1} unreliable, and so it is re-estimated by comparing it against the currently undetermined F_{i+2} . Both the widths of F_{i+1} and F_{i+2} are optimised using normalised cross-correlation. This process is demonstrated in Fig. 7. Note the width of the second frame of the woman shot has been correctly estimated although it is more than 10% narrower than the keyframe.

5 Conclusions and Future Work

In this paper we have shown the feasibility of a primarily automatic method for recovering the contents of lost films from source acetate rolls by performing a virtual unrolling of a 3D tomographic scan of the film. Our approach involved first generating the film reel by extracting lines (intensity ridges) along the film layers, connecting disconnected lines, aligning the lines from across the X-ray scans, and finally projecting densities along normals to the lines to measure the response of the silver content in the film. Finally, frames were extracted from the film reel, and reassembled into a video. Difficulties were encountered in the final stage due to stretching artifacts in the alignment stage of the virtual unrolling. Nevertheless, reasonable results were obtained, which could be improved in the future by better flattening methods.

The success of recovering this short section of film from a tomographic scan gives hope for recovery of large, damaged film reels. Unfortunately, the X-ray dose requirement increases dramatically with increasing size, so upscaling is problematic and even impossible to the degree that would be necessary for recovery of a 30cm diameter film reel. Not only would it be necessary to increase the detector array size to around 20,000 pixels across, but the number of recorded photons per pixel would also have to increase by thousands. This would require an, as yet unconceived of, detector with a massive dynamic range. Furthermore, acquiring such a photon count in a reasonable amount of time would require such an intense X-ray beam that heating would be a problem, bearing in mind that any dimensional change should be much less than 1 in 20,000. Conceivably, the smallest 8mm reels might be able to be scanned in one go, whereas larger film reels would need to be cut into smaller pieces. An alternative might be tomosynthesis, which would avoid the necessity of an X-ray path that passes diametrically through the film; however it is unlikely that this could produce a reconstructed image of sufficient quality.

Returning to the rediscovered episode of ‘The Morecambe and Wise Show’, its rapid degradation, along with the above limitations, meant that the only feasible solution was to cut the film into smaller sections which could then be scanned using the MuCAT 2 X-ray microtomography scanner at QMUL. Fig. 8 shows a single image from one such section. The quality is significantly poorer than the Snow White scan, as it contains many holes and also some local deformations. We are just starting to work on this more challenging data, and we believe that

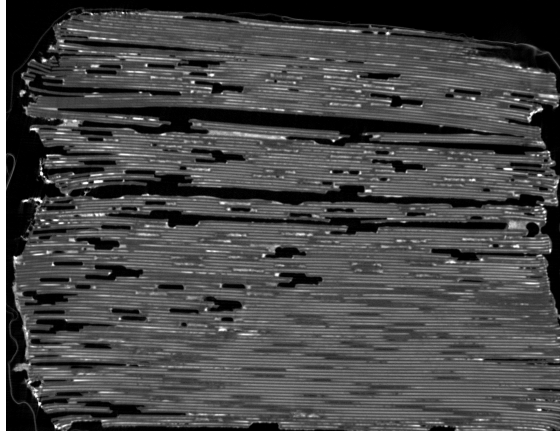


Fig. 8. An X-ray image of a section of ‘The Morecambe and Wise Show’.

our processing pipeline can cope since it was adapted from the pipeline developed for damaged historical scrolled parchments [10, 8], and that these documents also contained many artifacts such as holes, delaminations, geometric distortions, etc.

Acknowledgments. We thank Paul Vanezis (BBC) and Ulrich Reudel (BFI).

References

1. M. Binder. *A Light Affliction: A History of Film Preservation and Restoration*. Lulu.com, 2015.
2. G.R. Davis, A.N.Z. Evershed, and D. Mills. Quantitative high contrast X-ray microtomography for dental research. *Journal of Dentistry*, 41(5):475–482, 2013.
3. G.R. Davis and D. Mills. Brute force absorption contrast microtomography. In *Proc. SPIE: Developments in X-Ray Tomography IX*, volume 9212, 2014.
4. A. Macchia *et al.* Characterization and weathering of motion-picture films with support of cellulose nitrate, cellulose acetate and polyester. *Procedia Chemistry*, 8:175 – 184, 2013.
5. T. Freeth *et al.* Decoding the ancient Greek astronomical calculator known as the Antikythera Mechanism. *Nature*, 444:587–591, 2006.
6. L. Enticknap. *Film Restoration: The Culture and Science of Audiovisual Heritage*. Palgrave Macmillan, 2013.
7. A.C. Kokaram. *Motion Picture Restoration: Digital Algorithms for Artefact Suppression in Degraded Motion Picture Film and Video*. Springer, 2013.
8. C. Liu, P.L. Rosin, Y.-K. Lai, and W. Hu. Robust segmentation of historical parchment XMT images for virtual unrolling. In *Digital Heritage*, 2015.
9. D. Mills, A. Curtis, G. Davis, P.L. Rosin, and Y.-K. Lai. Apocalypto: revealing the Bressingham roll. *Journal of Paper Conservation*, 15(3):14–19, 2014.
10. O. Samko, Y.-K. Lai, D. Marshall, and P.L. Rosin. Virtual unrolling and information recovery from scanned scrolled historical documents. *Pattern Recognition*, 47(1):248–259, 2014.
11. C. Steger. An unbiased detector of curvilinear structures. *IEEE Transactions on Pattern Analysis and Machine Intelligence*, 20(2):113–125, 1998.